Available on CMS information server

CMS DN -2014/041

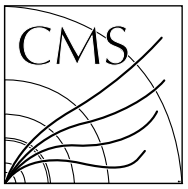

The Compact Muon Solenoid Experiment

Detector Note

The content of this note is intended for CMS internal use and distribution only

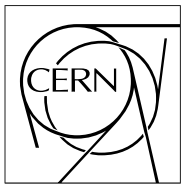

21 November 2014 (v3, 27 October 2015)

Post LS1 synchronisation of the CSC trigger primitives arriving at the CSC track finder

B. Michlin, D. Acosta, K. Banicz, P. Bortignon, M. De Gruttola, P. Everaerts, I. Furic, E. Juska, M. Ignatenko, A. Madorsky, P. Padley, J. Rorie, D. Williams, L. Uvarov

Abstract

The synchronisation of the CSC trigger primitives (Local Charged Tracks) at the CSC Track Finder is a part of the commissioning activities. To ensure that the Track Finder is operating at maximum efficiency, trigger primitives originating from the same muon must arrive at the Track Finder in the same BX. There are many sources of asynchronous delays of Local Charged tracks between the CSC chambers and the CSC Track Finder must be therefore corrected for. A synchronisation of the trigger primitives improves the trigger efficiency, the quality of the muon tracks, and reduces the trigger rate from background noise. A detailed method of synchronisation is presented showing typical results from cosmic ad beam data taken during the 2015 commissioning period. This note will provide a template to be followed for future synchronisation purposes.

1 Introduction and Motivation

The synchronization of the CSC trigger primitives at the CSC Track Finder (CSCTF) is a part of the trigger commissioning. The Track Finder (TF) can identify muon candidates using CSC trigger primitives (Local Charged Tracks) coming from the same bunch crossing (BX). Explicitly, if Local Charged Tracks (LCTs) produced by the same muon are not with in $\pm 1BX$, then an accurate track can not be made. There are several sources of asynchronous delays of LCTs between the CSC chambers and the CSCTF that must be corrected for. Major sources of asynchronizations include the signal propagation time across a CSC chamber and time-of-flight (TOF) corrections for the muon. A synchronization of the trigger primitives at the Track Finder, accounting for known and unknown sources of error and asynchronization improves the trigger efficiency, the quality of the muon tracks, and reduces the trigger rate from background noise.

A detailed synchronization study was performed during the CMS commissioning in 2009 [1], before the first run of the LHC. During Long Shutdown 1 (LS1) CSC on-chamber electronics were upgraded and installed for ME1/1, and an entirely new ring of CSC chambers (ME4/2) was added. See reference [2] for an explanation of the CSC detector layout and geometry. Because of these upgrades, a new synchronization study is needed, and has been performed, before the start of the next LHC physics run to ensure the optimal functionality of the CSCTF. The 2015 synchronization study has been performed using data collected during the Mid Week Global Runs (MWGR), the Extended Cosmic Run (ECR), and the first runs with stable beams at $\sqrt{s} = 13$ TeV at both 0 and 3.8 T.

This note focuses on the methods used in the synchronization of the CSCTF LCTs, and illustrates the typical behavior that may be expected to be seen under various data taking conditions. Data are collected in local runs using only CSC triggers, and global runs using the full Level-1 trigger. Specifically, a Cosmic RUn at ZEro Tesla (CRUZET) local run, and a collisions run at $\sqrt{s} = 13$ TeV at 3.8 T global run are the focal point of this note. However, the methods presented are suitable, and have been used, to verify the CSCTF LCT timing from beam halo data, beam splash data, collisions runs at 0 T, and all other runs associated with the TF and LHC commissioning activities.

Section 2 discusses the main sources of timing corrections that must be accounted for. Section 3 describes the two synchronization methods considered: a numeric procedure, and an analytic (matrix) procedure. Section 4 presents the results of the synchronization of the CSCTF LCTs for the 2015 Cosmic Run at ZEro Tesla (CRUZET), and an early 13 TeV stable collisions run at 3.8 Tesla.

2 Timing Corrections

The main timing corrections considered during synchronization account for the TOF of the muon from which the resulting LCTs are created, and for the propagation of the incident muon signal as it crosses the CSC chamber to the AFEB.

2.1 Time-of-Flight

The TOF correction applies exclusively to cosmic muons, since this correction factor is already taken into account for accelerator muons. Generally, the TOF between multiple LCTs created by the same cosmic muon must be corrected for at the CSCTF. This is performed by assuming that the muon is traveling at the speed of light, and in a straight line between the positions of the LCTs. However, when LCTs arrive at the Track Finder, there is already a TOF correction that has been implemented which assumed that the muon originated from the interaction point

(IP). For physics running, this is a valid assumption. Given the fact that the CSCTF LCTs need to be synchronized before the beginning of collisions, much of the data used comes from the commissioning period. Initially, CMS used cosmic data for detector commissioning. This means that the synchronization of the LCTs must be performed, mainly, using cosmic ray data (Cosmic Run At Four Tesla (CRAFT) and CRUZET). In the case of cosmic rays, an incident muon is more likely to be traveling towards the interaction point, rather than away from it. Therefore, the initial collision TOF correction made to the LCTs must be uncorrected for (since the timing may have been corrected in the wrong direction), and then the correct TOF must be applied. Thus, before a TOF correction can be added, it must be determined which direction a muon is traveling: forwards (away from the IP), or backwards (towards the IP).

Three requirement to determine direction,how do meet them?

In order to determine the direction of an incident cosmic muon a strict event selection must be applied. It is required that there is exactly one LCT in ME2 and exactly one LCT in ME3. This is because for the cosmic runs, the CSCs only trigger on the bottom of ME2 and ME3 in ϕ, i.e.: trigger sectors 4, 5, and 6 in the positive endcap, and trigger sectors 10, 11, and 12 in the negative endcap. It is also required that there are exactly two LCTs found in neighboring chambers in the CSC ring that is to be synchronized; if an event has three LCTs in the CSC ring that is to be synchronized, the event is rejected. These cuts are designed to reduce the ambiguity regarding the path of the incident muon. For example, if there is one LCT in ME2 and one LCT in ME3 but three LCTs in ME1/1 (two LCTs from neighboring chambers and a third LCT elsewhere in ME1/1) then there is ambiguity as to which of the LCTs in ME1/1 should be aligned to the triggering LCT, and which is from background noise or an unassociated muon. It is important to note that this particular event selection is very restrictive and is used in all cases where the TOF correction is applied at the CSCTF for synchronization purposes. Lastly, it is required that the LCTs in ME2 and ME3 are registered in the triggering, central, bunch crossing, $BX = 6$. Adding this final cut in to the event selection will help to provide events in which the chambers being synchronized are being synchronized to the triggering, central, BX. The event selection criteria also help to reduce noise by helping to guarantee that the LCTs being used come from an actual cosmic muon.

Finally, to determine the direction of an incident cosmic muon, the y-position of the LCTs in ME2 and ME3 are compared where the y coordinate corresponds to the vertical with respect to the LHC plane, the z coordinate is along the beam axis, and the x coordinate points towards the center of the LHC ring. Since the cosmic muons are coming from above, if the LCT in ME3 has a higher y-position than the LCT in ME2, then the muon which created the LCTs is likely backwards moving. Similarly, if the LCT in ME2 has a higher y-position than the LCT in ME3, the muon is likely forwards moving. When the actual TOF is being calculated it is calculated between two of the three LCTs. The TOF calculation uses the LCT in the station to be synchronized (generally ME1/1 or ME4/2) and the LCT with the higher y-position (ME2 or ME3) [3]. The expected TOF is then complemented (for forward moving muons) or counteracted (for backwards moving muons) by the pre-existing TOF correction, so the CSCTF LCT BXs are adjusted appropriately. Figure 1 shows the expected TOF correction (which is already applied before the LCT reaches the CSCTF) and the actual TOF from a cosmic muon.

2.2 Signal Propagation Time

The signal propagation time refers to the time that it takes for the signal (created by an incident muon) to propagate across an anode in the CSC chamber to the AFEB where the timing information is first assigned. This correction may seem minuscule (on the order of a nanosecond), but must be accounted for. This is because, for muons that pass through the overlap region of a CSC chamber (which are exclusively used for this analysis) two signals are created which

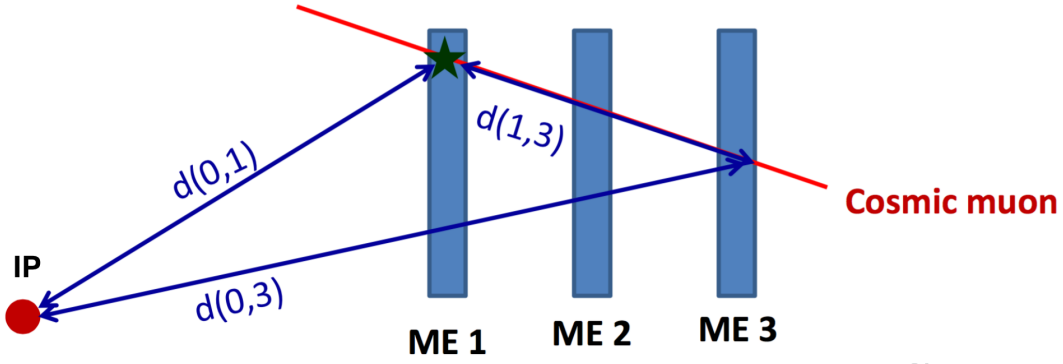

Figure 1: Here, d(0,3)-d(0,1) is the expected TOF difference between the two LCTs, while d(1,3) is the actual time difference between the LCTs for a cosmic muon, and IP is the interaction point. From this, the actual TOF may be calculated and applied. [3]

have a maximal propagation time difference. Explicitly, the two signals from the LCTs created in the overlapping region of two CSC chambers are necessarily close to one AFEB, and on the opposite side to the other AFEB. This can be seen clearly from Figure 2.

The correction for the signal propagation time difference between two LCTs created in the overlap region from the same muon is estimated by using the wiregroup and halfstrip information contained in the LCT. By using the geometry of the CSCs, the distance from the LCT position to the AFEB may then be determined. It is then assumed that the signal travels across the anode at the speed of light. Although this timing affect from the signal propagation is on the scale of a few nanoseconds this is of the same scale as the CSCTF LCT synchronization timing correction to be determined, and therefore, it may not be neglected.

3 Synchronization Methods for the CSC Muon System

The two following methods of synchronization that are presented make use of the development and subsequent minimization of a chi-squared function. The chi-squared includes all of the necessary CSCTF LCT timing data and, when minimized, yields an optimal solution for the timing adjustments for each of the individual chambers in order to produce a synchronized CSC ring. The chi-squared is minimized both numerically using MINUIT2 [4] in ROOT [5] and analytically via a matrix equation. By using both methods of minimization an internal check is performed on the resulting synchronization timing corrections and additional confidence may be placed on the results.

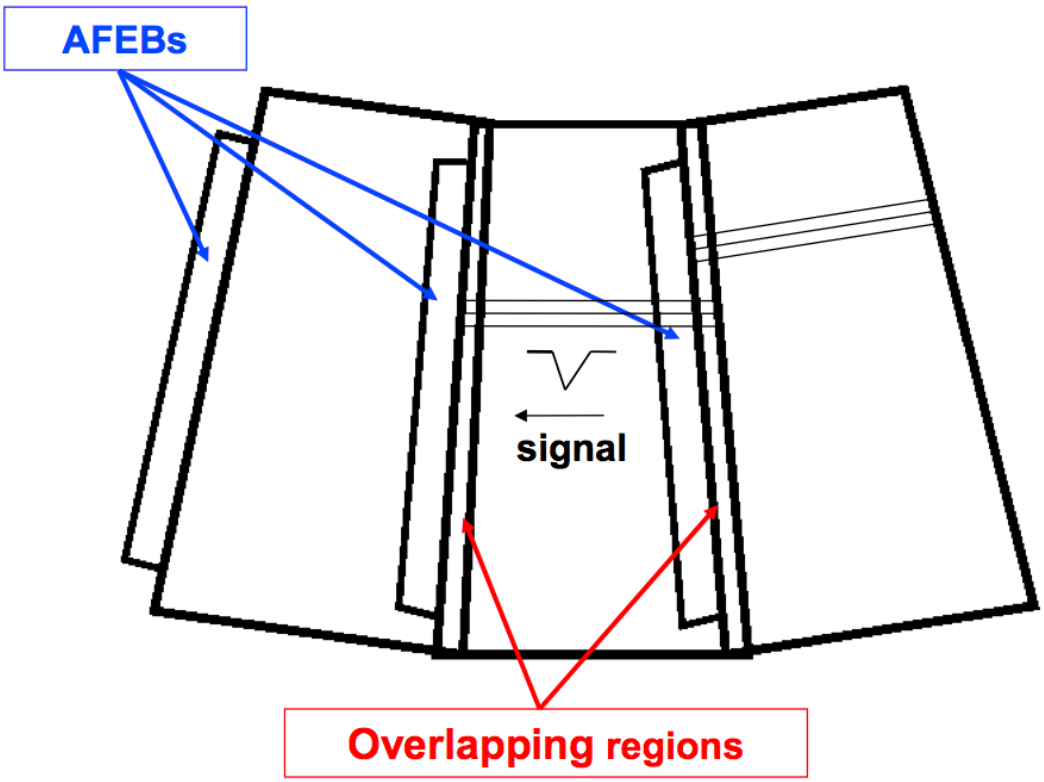

Figure 2: Neighboring CSC chambers showing the overlap region. [1]

In order to investigate and implement these synchronization methods events in which there are LCTs in neighboring chambers in the CSC ring to be synchronized are exclusively used. The assumption is that the LCTs in neighboring chambers originate from the same muon that has passed through the overlapping region between them. Figure 2 shows the overlapping regions between neighboring CSC chambers. These muons that have passed through the overlap region between neighboring CSC chambers should produce LCTs which have the same BX timing information as seen by the CSCTF. In the case that they do not, the results may be compared and the chamber timing information may be adjusted as necessary. Thus, by comparing and modifying the timing information from all sets of neighboring chambers, a CSC ring may be successfully synchronized.

3.1 Development of Chi-Squared

Reference [1] recommends developing a chi-squared function which includes all of the timing information for all of the CSC chambers in a ring along with a floating timing correction parameter for each chamber. Minimizing the chi-squared function with respect to the floating timing correction variables will then yield an optimal solution for the synchronization timing corrections that can then be applied individually to each respective chamber. This method has been found to produce accurate results and can reliably synchronize a CSC ring.

The development and subsequent minimization of the chi-squared function uses data that has already been corrected for TOF (for cosmic runs) and signal propagation time (for all runs). It is critical to note that any other unknown sources of errors and asynchronizations will also be corrected for with this method.

3.2 CSC Ring Synchronization via Chi-Squared Minimization

The synchronization function used for the 2015 commissioning is defined as

$$\chi^2 = \sum_n \left(\frac{\Delta_n - \Delta_{n+1} + m_{n,n+1}}{\sigma_{n,n+1}} \right)^2, \tag{1}$$

where the index n runs over all chambers in the ring (and $n+1$ is the neighboring chamber to chamber n), $m_{n,n+1}$ is the difference between the mean of the LCT BX distribution of chambers n and $n+1$, $\sigma_{n,n+1}$ is the uncertainty on $m_{n,n+1}$, and Δ_n and Δ_{n+1} are the synchronization timing corrections to be determined for chambers n and $n+1$ respectively. The optimal synchronization timing corrections are then determined by minimizing equation 1 where there is a floating, non-independent, Δ variable for each chamber. It should be noted that for the final chamber in the ring (chamber number 36 or 18 depending on which CSC ring is being synchronized) the neighboring chamber, with index $n+1$, is 1. In this way, equation 1 can encompass all of the information necessary to describe the timing of an entire CSC ring. Once found via minimization, the respective timing correction is applied to the appropriate chamber, yielding an optimally synchronized ring.

3.3 Numerical Minimization

Using the input values from the experimental data, equation 1 may be written explicitly. Once in this form, the optimal synchronization timing corrections (Δ_n) may be determined via minimization. The minimization is performed numerically using MINUIT2 [4] where the output is the Δ_n values for each chamber. It should be noted that when there are no events which pass the event selection for individual chambers, the terms are skipped when creating equation 1. If statistics are too low and no LCTs are found in either of the overlap regions of a chamber then the corresponding timing correction is omitted from the numerical minimization and the results. For example, if there are no LCTs found in the overlap region between chambers 1 and 2, or 2 and 3, the correction Δ_2 would be completely omitted from the results. If this occurs, then the CSC ring is no longer a "ring" because it will have a gap in the synchronization. If this occurs twice then the CSC ring is essentially split into two distinct systems. If this happens, then it is equivalent to synchronizing the two pieces independently, and the end result may not have the two pieces synchronized to each other. This can lead to unrealistic uncertainties and unreliable results. Although, as long as the initial timing of the CSCTF LCTs is within reason, this is still a viable method of estimating the required synchronization constants. The case of low statistics is uncommon when using beam data, however, the problem has been seen to arise when using individual global or local cosmic runs.

Because of the nature of how the chi-squared function is derived, the minimum is insensitive to many influences. For example, if every chamber is shifted uniformly, this will not be detected by minimizing the chi-squared. Thus, an infinite number of minima exist for equation 1. This means that a minimum will always be found regardless of the seed value input to MINUIT2. To mitigate the influence of this issue, MINUIT2 is run over a range of seed values between -10 and 10 with a step-size of 0.01. The smallest of the determined minima is used for synchronization purposes. In practice, however, the differences between the minima do not have a noticeable affect on the determined timing shifts, and the differences between the solutions are well below the resolution of the CSC chambers, CSCTF timing capabilities, and the uncertainties on the results.

The synchronization corrections obtained from the minimization of equation 1 may then be

used to adjust the timing information for each chamber individually. Since the minimum of the chi-squared is not influenced by constant shifts of the timing corrections, the timing corrections are adjusted such that each chamber is corrected by the smallest amount possible without influencing the relative differences between the timing corrections. In practice, this means that the average of the timing corrections is deducted from each individual timing correction.

3.4 Matrix Minimization

Analytically, minimizing the chi-squared function in equation 1 can be done by taking the derivative of equation 1 with respect to Δ_i and setting the result equal to zero:

$$\frac{\partial \chi^2}{\partial \Delta_i} = \frac{-2(m_{i-1} + \Delta_{i-1} - \Delta_i)}{\sigma_{i-1}^2} + \frac{2(m_i + \Delta_i - \Delta_{i+1})}{\sigma_1^2} = 0. \tag{2}$$

Rearranging equation 2 gives:

$$-\sigma_i^2 \Delta_{i-1} + (\sigma_{i-1}^2 + \sigma_i^2)\Delta_i - \sigma_{i-1}^2 \Delta_{i+1} = \sigma_i^2 m_{i-1} - \sigma_{i-1}^2 m_i. \tag{3}$$

Including the number of chambers, n, equation 3 can be organized into a matrix equation

$$\underbrace{\begin{bmatrix} \sigma_n^2 + \sigma_1^2 & -\sigma_n^2 & 0 & \cdots & 0 & -\sigma_1^2 \\ -\sigma_2^2 & \sigma_1^2 + \sigma_2^2 & -\sigma_1^2 & 0 & \cdots & 0 \\ \vdots & \vdots & \ddots & \ddots & \ddots & \vdots \\ -\sigma_{n-1}^2 & 0 & \cdots & 0 & -\sigma_n^2 & \sigma_{n-1}^2 + \sigma_n^2 \end{bmatrix}}_{A} \underbrace{\begin{bmatrix} \Delta_1 \\ \vdots \\ \vdots \\ \Delta_n \end{bmatrix}}_{\Delta} = \underbrace{\begin{bmatrix} \sigma_1^2 m_n - \sigma_n^2 m_1 \\ \vdots \\ \vdots \\ \sigma_n^2 m_{n-1} - \sigma_{n-1}^2 m_n \end{bmatrix}}_{b}. \tag{4}$$

Equation 4 can then be written as $A\Delta = b$. Recall that since the chambers form a ring, chambers 1 and n are neighbors when n is either 18 or 36 depending on the number of chambers in the ring being synchronized.

The rows of the matrix A are not independent, so this equation has no unique solution [6] (which was similarly concluded for the numeric minimization). A solution may still be found using the Moore-Penrose pseudoinverse [6]: a generalization of the matrix inverse that can be calculated using the TDecompSVD [7] class in ROOT [5]. Labelling the pseudoinverse of A as $A^\dagger$, the general solution of equation 4 can be written as:

$$\Delta = A^\dagger b + (I - A^\dagger A)w, \tag{5}$$

where w is an arbitrary vector [6]. Since any shift to a solution Δ will still synchronize the chambers, w can be set to 0 for simplicity, giving the solution:

$$\Delta = A^\dagger b. \tag{6}$$

Once the pseudoinverse, $A^\dagger$, is calculated the timing constants may be written explicitly:

$$\Delta = \begin{bmatrix} A^{\dagger}_{1,1}(\sigma_1^2 m_n - \sigma_n^2 m_1) + A^{\dagger}_{1,2}(\sigma_2^2 m_1 - \sigma_1^2 m_2) + \cdots \\ A^{\dagger}_{2,1}(\sigma_1^2 m_n - \sigma_n^2 m_1) + A^{\dagger}_{2,2}(\sigma_2^2 m_1 - \sigma_1^2 m_2) + \cdots \\ \vdots \end{bmatrix}. \tag{7}$$

Because m_i, σ_i^2, and $A^{\dagger}_{i,j}$ are all experimental values, equation 7 provides a nominal value for the timing synchronization constant for each chamber in a CSC ring.

Appendix A shows a complimentary derivation using a matrix minimization method suggested by the Particle Data Group [8]. This method yields a result identical to equation 7, thus confirming the results found and all of the assumptions made.

3.4.1 Error Propagation

Unlike the numeric minimization, when determining the synchronization timing corrections analytically the nominal result and the error must be determined individually. To demonstrate the process of propagating the uncertainty through the matrix minimization method the error calculation for the timing synchronization constant of chamber 1 is presented explicitly, after which, a general result shown.

Beginning by rearranging the expression for the first timing constant Δ_1 from equation 7 gives:

$$\Delta_1 = m_1(A^{\dagger}_{1,2}\sigma_2^2 - A^{\dagger}_{1,1}\sigma_n^2) + m_2(A^{\dagger}_{1,3}\sigma_3^2 - A^{\dagger}_{1,2}\sigma_1^2) + \cdots . \tag{8}$$

The error propagation equation for an arbitrary function $x = f(u, v, ...)$ can be written as

$$\sigma_x^2 = \sigma_u^2(\frac{\partial x}{\partial u})^2 + \sigma_v^2(\frac{\partial x}{\partial v})^2 + \cdots + 2\sigma_{uv}^2(\frac{\partial x}{\partial u})(\frac{\partial x}{\partial v}) + \cdots \tag{9}$$

where σ_x^2 is the variance of the function x, σ_u^2 is the variance of the variable u, and σ_{uv}^2 is the covariance between u and v [9]. In equation 8, Δ_1 is written as a function of m_i, i.e.: $\Delta_1 = f(m_1, m_2, ...)$. Using this fact, equation 9 can be rewritten with $x = \Delta_1, u = m_1, v = m_2, ...$ producing:

$$\sigma_{\Delta_1}^2 = \sigma_1^2(\frac{\partial \Delta_1}{\partial m_1})^2 + \sigma_2^2(\frac{\partial \Delta_1}{\partial m_2})^2 + \cdots + 2\sigma_{12}^2(\frac{\partial \Delta_1}{\partial m_1})(\frac{\partial \Delta_1}{\partial m_2}) + \cdots . \tag{10}$$

Calculating the covariance of the relative BX between chambers would require muons in the same event to pass through the overlap regions of multiple pairs of chambers in the same event, which is a very rare occurrence in a typical run. Therefore, calculating the covariance terms in equation 10 is difficult, if not impossible. In such cases it is a reasonable approximation to ignore the covariance terms [9], which then allows equation 10 to be written as

$$\sigma_{\Delta_1}^2 = \sigma_1^2(\frac{\partial \Delta_1}{\partial m_1})^2 + \sigma_2^2(\frac{\partial \Delta_1}{\partial m_2})^2 + \cdots . \tag{11}$$

Combining equations 8 and 11 provides

$$\sigma_{\Delta_1}^2 = \sigma_1^2(A^{\dagger}_{1,2}\sigma_2^2 - A^{\dagger}_{1,1}\sigma_n^2)^2 + \sigma_2^2(A^{\dagger}_{1,3}\sigma_3^2 - A^{\dagger}_{1,2}\sigma_1^2)^2 + \cdots \tag{12}$$

which is the equation for the variance of the timing synchronization constant for chamber 1 in terms of the variances of m_i (σ_i^2). σ_i^2 values may be determined experimentally for equation 12, and therefore, so may Δ_1.

Equation 12 may be made general to yield the result for the uncertainty on the determined nominal timing synchronization corrections:

$$\sigma_{\Delta_i}^2 = \sum_{j=1}^{n} \sigma_j^2 (A_{i,j+1}^{\dagger} \sigma_{j+1}^2 - A_{i,j}^{\dagger} \sigma_{j-1}^2)^2. \tag{13}$$

Using the results presented in equations 7 and 13, the final result of the timing synchronization constant for chamber i calculated using the matrix minimization method can be written as $\Delta_i \pm \sigma_{\Delta_i}$. This result may then be used to adjust the timing information for each chamber individually, thereby synchronizing the CSCTF LCTs.

4 Results

4.1 Cosmic Muon Data

During the 2015 CMS commissioning period throughout the Mid Week Global Runs and the Extended Cosmic Runs cosmic data were taken with and without magnet (CRAFT and CRUZET). The procedure for working with and synchronizing this data is identical. RAW data should be taken and processed using the official L1Ntuple package[1] making sure that the CSCTF DIGIs are being processed. When working with global runs, it is important to apply a quality cut (quality > 10) on the LCTs. In addition, in processing and track making, the LCT list found in the resulting L1Ntuple may contain duplicate LCTs. It is important to only work with "unique" LCTs.

4.1.1 CRUZET

In order to find the CSCTF LCT synchronization timing corrections equation 1 must be created and minimized. To do this, the variables $m_{n,n+1}$ and $\sigma_{n,n+1}$ must be determined from the experimental data. This procedure will be shown explicitly for ME+1/1 for CRUZET local run 227021 taken during the 2015 commissioning period. As with nearly all cosmic runs, single LCTs from the bottom of stations ME2 or ME3 were used for triggering purposes. To begin, we look at the distribution of the CSCTF BX without any restrictions, shown in Figure 3a. This plot is made by first plotting the BX value for each individual unique CSCTF LCT for each chamber, and then using the mean from each plot as a point in Figure 3a. The plot shows a fit of a polynomial of degree-zero since the CSCTF LCT BX is expected to fall on a straight horizontal line at 6 (the central BX). However, a strong sinusoidal behavior is seen, and expected, for cosmic muons. This behavior is largely due to the directional bias of cosmic rays as discussed in section 2.1, and is nearly completely eliminated by applying the TOF correction as shown in Figure 3b. Recall that applying the TOF correction requires a change in event selection such that there is exactly one LCT in ME+2 and ME+3, and exactly two neighboring LCTs in the ring to be synchronized, here ME+1/1. Therefore, the data shown in Figure 3b are a subset of the data shown in Figure 3a. The final correction made to the CSCTF LCTs is the signal propagation correction, discussed in section 2.2. The result of the signal propagation time is extremely small, as to be expected, and is on the order of 1 ns (0.04 BX). Figure 3c shows the CSCTF LCT BX including the signal propagation time correction in conjunction with the TOF correction. Although the

[1] https://twiki.cern.ch/twiki/bin/viewauth/CMS/L1TriggerDPGNtupleProduction

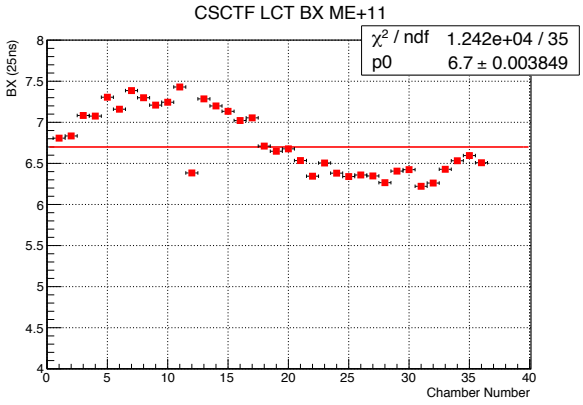

(a)

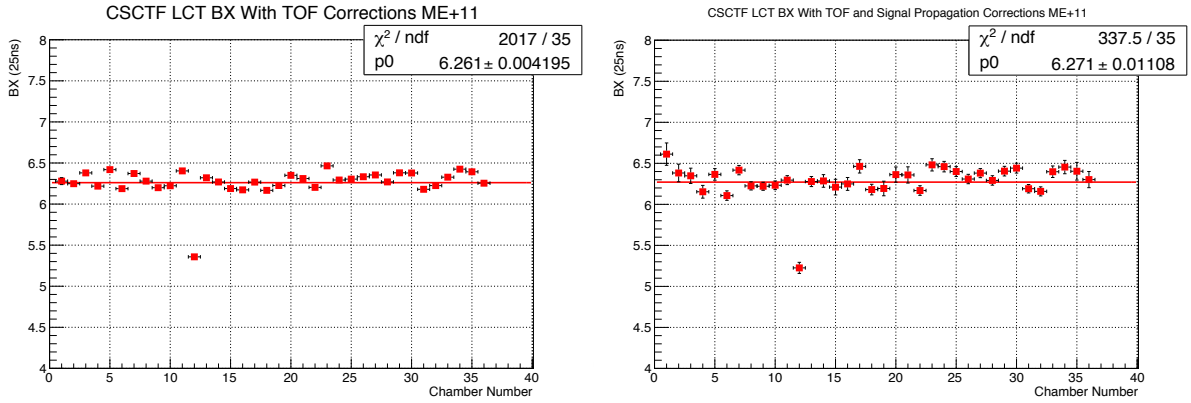

(b) (c)

Figure 3: (a): The CSCTF LCT BX for ME+1/1 for each chamber with no corrections altering the data is shown for CRUZET local run 227021. A strong sinusoidal behavior is clearly present. (b): The CSCTF LCT BX for ME+1/1 for each chamber including the TOF correction is shown for CRUZET local run 227021. The TOF adjustment corrects the sinusoidal behavior. (c): The CSCTF LCT BX for ME+1/1 for each chamber including the TOF and signal propagation corrections is shown for CRUZET local run 227021. A small improvement from the TOF correction, but a more accurate fit is seen.

affect is small, note that the fit to the data is improved. Also note that even at this early stage it is possible to see that one chamber, chamber 12, is not synchronized with the others.

The next step is to look at the CSCTF LCT BX of LCTs falling only in the overlapping region between chambers, since this is the data that is used in the chi-squared function shown in equation 1. This is done by only plotting the CSCTF LCT BX for LCTs falling in neighboring chambers after the TOF and signal propagation corrections have been applied. Again, the mean is extracted for each set of overlapping chambers and the relative BX ($BX_n - BX_{n+1}$) between the LCTs can be found. Figure 4 demonstrates this process for ME+1/1 from CRUZET local run 227021, and shows the CSCTF LCT BX timing for LCTs from overlapping chambers (n and $n+1$) with the TOF and signal propagation corrections applied. Note that since the TOF and signal propagation corrections have been made, the previous event selection persists. If Figure 4 showed data from an already synchronized ring, it would be expected that the relative BX points should all fall precisely at zero. This is because for LCTs coming from the same muon which passes through the overlapping region of two chambers, the timing information at the CSCTF should be identical, leading to a relative BX of zero. Additionally, the misalignment

of chamber 12 is evident by the fact that both of the overlapping regions (the overlap region between 11 and 12, and 12 and 13) have a large relative BX.

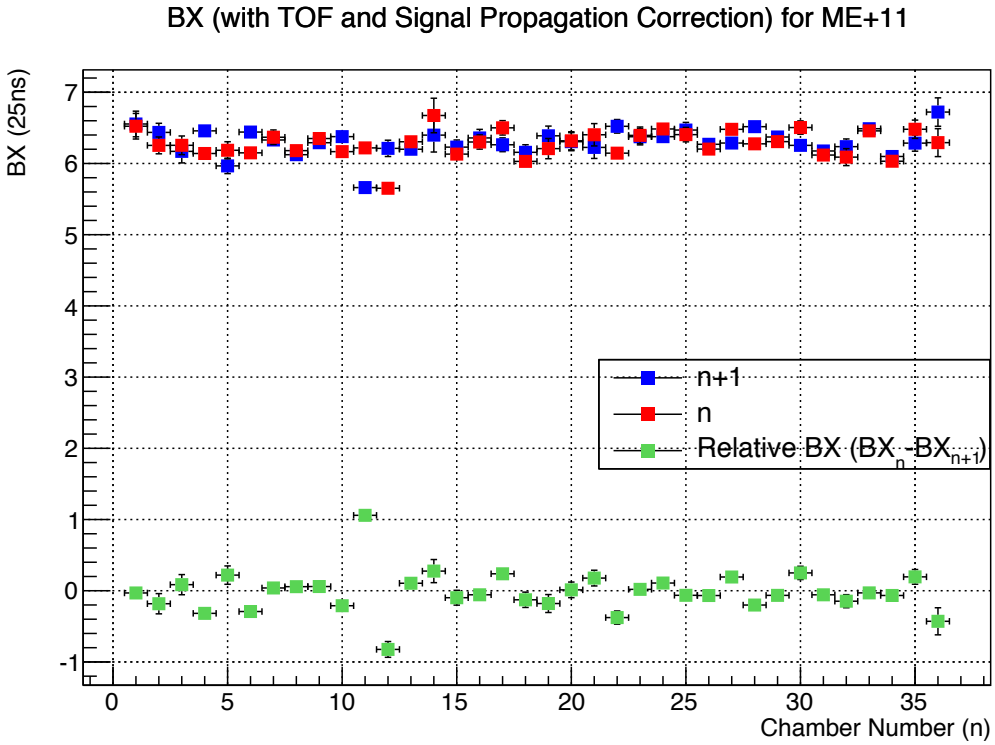

Figure 4: The CSCTF LCT BX timing for all of the overlapping chambers of ME+1/1 including the TOF and signal propagation corrections is shown for CRUZET local run 227021. Here, n runs over all 36 chambers of ME+1/1 and the green points are the relative BX values for each overlap region ($BX_n - BX_{n+1}$). Each bin shows the mean timing of the LCTs from that chamber overlap region (red points), the timing of the neighboring chamber for LCTs in the same overlap region (blue points), and the difference between the two (green points). This means that for bin 5 ($n = 5$), the overlap region between chambers 5 and 6 is shown where chamber 5 is the red point and chamber 6 is the blue point. In the next bin, 6 ($n = 6$), the overlap region between chambers 6 and 7 is shown where chamber 6 is the red point and chamber 7 is the blue point. In this way, the entire CSC ring timing information is included. Note that for $n = 36$, $n + 1 = 1$.

Figure 4 encompasses all of the timing information necessary to create equation 1, therein allowing the timing constants necessary to synchronize the CSCTF LCTs from ME+1/1 to be found. As applied to equation 1, explicitly, $m_{n,n+1}$ are the green points from Figure 4 and $\sigma_{n,n+1}$ are the y-error bounds on those points. The y-error bounds on the relative BX originate from the standard error from the mean of the BX for each overlap region (the uncertainty on the points n and $n + 1$). Since the relative BX is found via simple subtraction, propagating the error is trivial. With this information, the chi-squared function (equation 1) may be constructed explicitly.

With the chi-squared function constructed, the next step is to determine the timing correction values (Δ_n) via minimization. Following the procedures outlined in sections 3.3 and 3.4 the timing corrections may be determined. These values are shown in Table 1 as determined both by matrix equation and by numerical minimization. The timing corrections determined by both minimization methods have identical nominal values with slight variation in the uncertainty. The largest correction found, 0.568 BX (∼14 ns), is to be applied to chamber 12. Applying the

corrections yields the optimally synchronized CSCTF LCT BXs for ME+1/1, shown in Figure 5 for all chamber overlap regions. Note that the CSCTF LCTs from ME+1/1 are nearly perfectly synchronized within uncertainty as evident by the relative BX falling precisely at zero. The only exception is chamber 12, as expected, and one of its neighboring chambers.

Chamber	Numerical Timing Correction	Matrix Timing Correction
1	−0.112 +/− 0.068	−0.112 +/− 0.175
2	−0.143 +/− 0.068	−0.143 +/− 0.175
3	−0.279 +/− 0.143	−0.279 +/− 0.176
4	−0.148 +/− 0.173	−0.148 +/− 0.172
5	−0.447 +/− 0.180	−0.447 +/− 0.170
6	−0.189 +/− 0.187	−0.189 +/− 0.164
7	−0.474 +/− 0.187	−0.474 +/− 0.163
8	−0.425 +/− 0.188	−0.425 +/− 0.161
9	−0.362 +/− 0.189	−0.362 +/− 0.161
10	−0.295 +/− 0.191	−0.295 +/− 0.160
11	−0.497 +/− 0.193	−0.497 +/− 0.161
12	0.568 +/− 0.195	0.568 +/− 0.161
13	−0.227 +/− 0.202	−0.227 +/− 0.163
14	−0.110 +/− 0.205	−0.110 +/− 0.164
15	0.225 +/− 0.206	0.225 +/− 0.164
16	0.152 +/− 0.202	0.152 +/− 0.163
17	0.097 +/− 0.202	0.097 +/− 0.163
18	0.348 +/− 0.206	0.348 +/− 0.163
19	0.247 +/− 0.213	0.247 +/− 0.163
20	0.104 +/− 0.217	0.104 +/− 0.161
21	0.144 +/− 0.216	0.144 +/− 0.159
22	0.349 +/− 0.213	0.349 +/− 0.156
23	−0.007 +/− 0.209	−0.007 +/− 0.154
24	0.029 +/− 0.205	0.029 +/− 0.152
25	0.146 +/− 0.203	0.146 +/− 0.151
26	0.090 +/− 0.201	0.090 +/− 0.150
27	0.032 +/− 0.199	0.032 +/− 0.150
28	0.239 +/− 0.197	0.239 +/− 0.151
29	0.049 +/− 0.195	0.049 +/− 0.151
30	−0.007 +/− 0.194	−0.007 +/− 0.152
31	0.262 +/− 0.190	0.262 +/− 0.155
32	0.220 +/− 0.186	0.220 +/− 0.157
33	0.093 +/− 0.180	0.093 +/− 0.160
34	0.078 +/− 0.172	0.078 +/− 0.162
35	0.014 +/− 0.172	0.014 +/− 0.163
36	0.233 +/− 0.164	0.233 +/− 0.168

Table 1: Timing corrections for CSCTF LCTs in BX units (25 ns). Results shown for both numerical and matrix minimization.

For completeness, the CSCTF LCT BX with TOF corrections, signal propagation, and timing synchronization corrections is shown for all CSCTF LCTs (not only those from the overlap regions) in Figure 6. After the application of the TOF, signal propagation, and synchronization corrections found via minimizing the chi-squared function, it would be expected that the resulting LCT BX should be constant over all chambers. However, the CSCTF LCT BX after TOF and synchronization corrections have been applied, although synchronized, has structure (also seen in Figure 5). The triggering region (bottom chambers, 18-36) shows the expected, flat, behavior, but the upper chambers (1-17) show a type of sinusoidal behavior. Because of the previously seen behavior shown in Figure 3a it is assumed that this behavior is an artifact of the geometry of cosmic muons and the trigger region bias. This is an example of an "unknown unknown" that this synchronization procedure is able to correct for, and this behavior is not expected, or seen, for accelerator muons as shown in section 4.2.

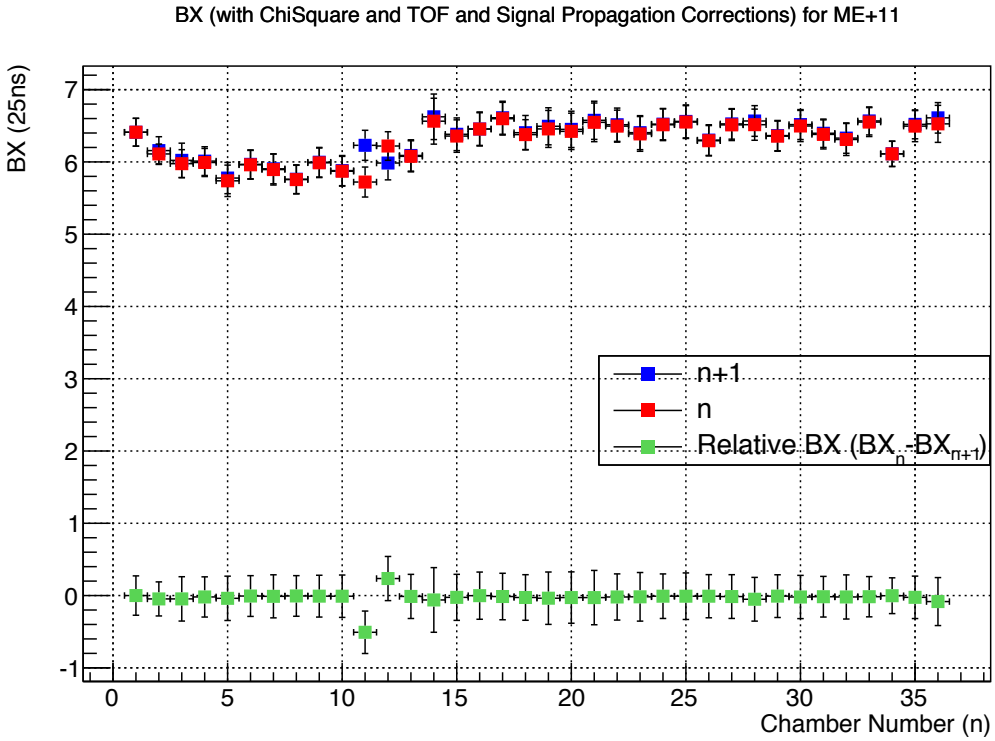

Figure 5: The CSCTF LCT BX for ME+1/1 for all sets of neighboring, overlapping, chambers including the TOF, signal propagation, and synchronization corrections from numerical minimization is shown for CRUZET local run 227021.

4.2 Stable 13 TeV Collisions

The procedure for analyzing and synchronizing collision data is much the same as cosmic data with two major differences. Recall that the existing LCT TOF correction (made for accelerator muons) had to be adjusted so that cosmic muons could be studied, as described in section 2.1. This correction no longer needs to be performed. Furthermore, this removes the necessity of applying the strict TOF event selection requiring exactly one LCT in ME2 and ME3 and exactly two neighboring LCTs in the CSC ring to be synchronized. The second difference is that since during collisions there are proton-bunch trains with high pileup, CSC chambers may record multiple LCTs from uncorrelated muons. Figure 7a clearly shows the 50 ns bunch trains appearing at CSCTF LCT BX 4 and 8, ± 2 BX (50 ns) from the central BX. This behavior is more apparent when compared to Figure 7b which shows the CSCTF LCT BX for a typical global CRUZET run where there are no proton-bunch trains (only cosmic muons). From experience with cosmic muons it is clear that the synchronization timing correction to be applied is on the order of a few ns, and not close to 50 ns. Therefore, a cut of ± 1 BX from the central BX is placed on the LCTs. Aside from these two differences there are no variations on the procedure for determining the synchronization timing corrections.

When analyzing collisions runs the results from only the certified lumisections[2] of global collisions run 251643 for ME+1/1 are shown. As expected, the sinusoidal behavior seen in the CSCTF LCT BX is no longer present since this behavior was due to the geometric bias from the cosmic muons, as shown in Figure 8. Furthermore, because of progress made in the LCT timing during the commissioning period, when stable beams began the CSCTF LCTs were nearly

[2]JSON file: Cert_246908-251883_13TeV_PromptReco_Collisions15_JSON_MuonPhys_v4.txt

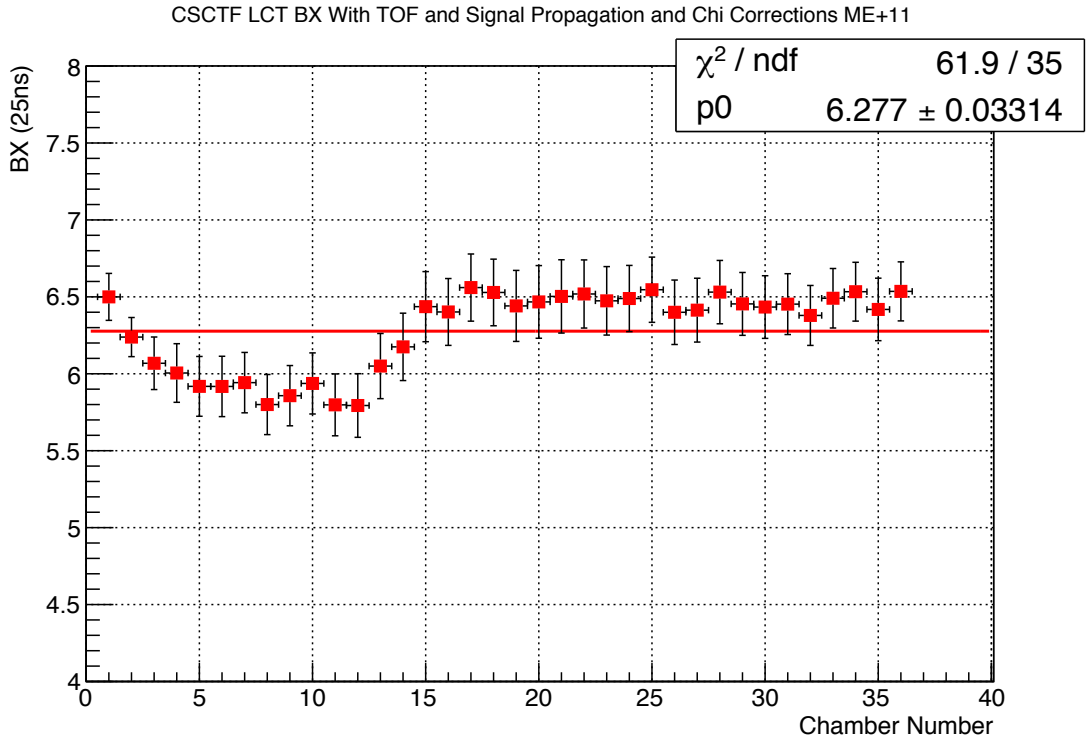

Figure 6: The CSCTF LCT BX for ME+1/1 for each chamber including the TOF, signal propagation, and synchronization corrections from numerical minimization is shown for CRUZET local run 227021.

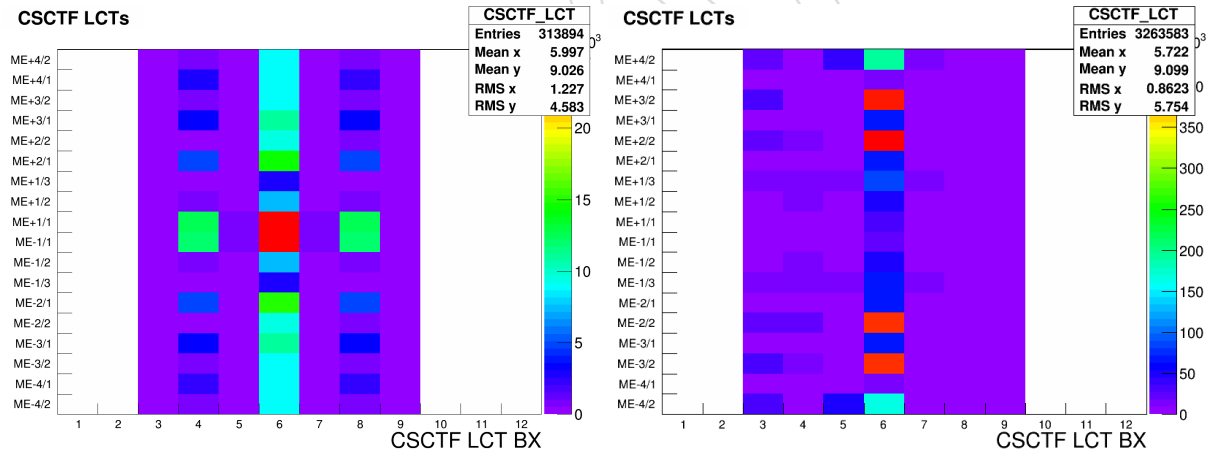

(a) (b)

Figure 7: (a): The CSCTF LCT timing from the online DQM for global collisions run 251643 which ran with 50 ns proton-bunch trains and a $\sqrt{s} = 13$ TeV at 3.8 T. (b): The CSCTF LCT timing from the online DQM for a typical global CRUZET run (237956).

exactly synchronized and aligned to the central BX before any adjustments were made, as displayed by Figure 9a. Synchronization may still be used for a fine-tuned adjustment, however, since the data is already consistent with being synchronized within the resolution of the Track Finder even before a signal propagation correction is applied no adjustments are required. Figure 9b shows the detail of the relative BX from Figure 9a including a fit using a polynomial of

330 degree-zero. The data is seen to be consistent with being completely synchronized, with a fit
331 consistent with zero.

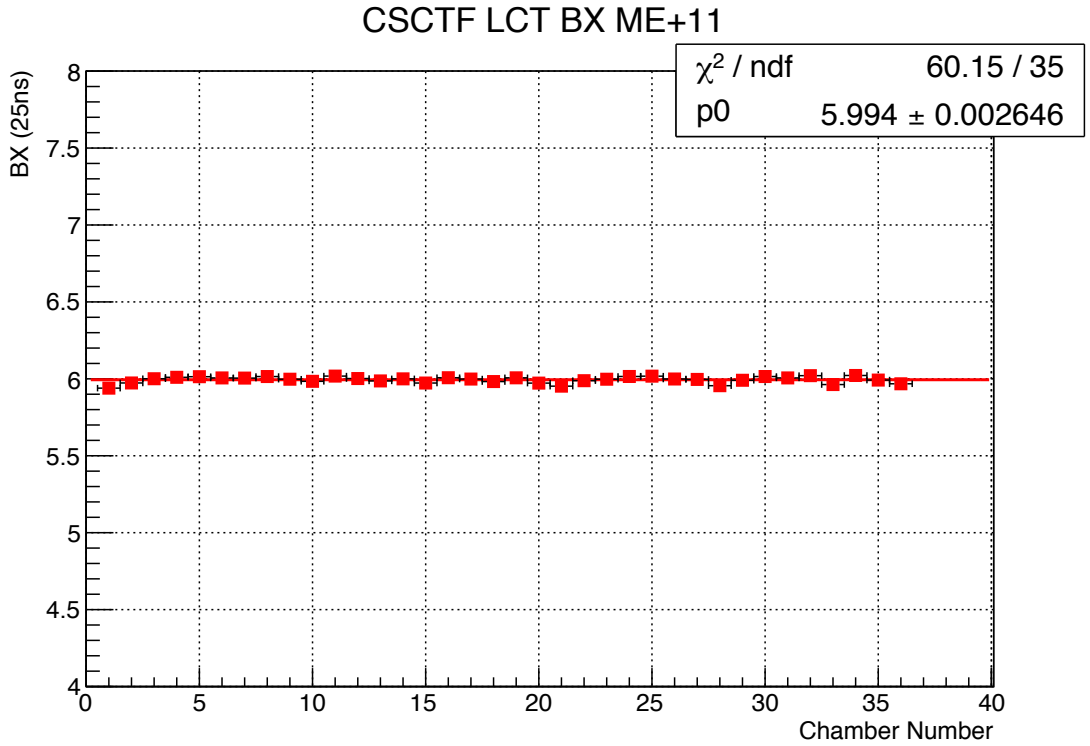

Figure 8: The CSCTF LCT BX for ME+1/1 for each chamber with no corrections adjusting the data for global collisions run 251643.

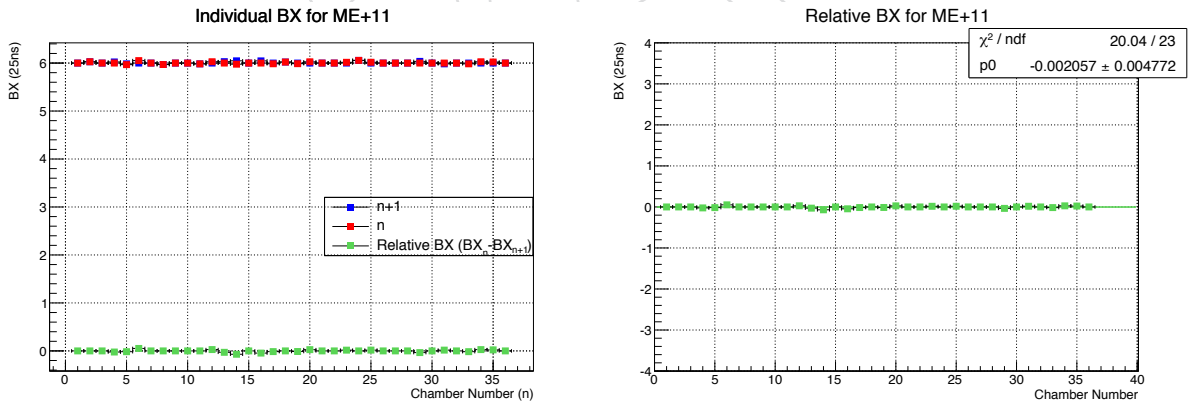

(a) (b)

Figure 9: (a): The CSCTF LCT BX for ME+1/1 for neighboring chambers with no corrections adjusting the data for global collisions run 251643. (b): The CSCTF LCT relative BX for ME+1/1 for neighboring chambers with no corrections adjusting the data for global collisions run 251643. A fit of polynomial degree-zero is shown and is consistent with zero within uncertainty.

5 Conclusions

A numerical method and an analytic method of synchronizing the CSCTF LCTs at the Track Finder have been developed and presented. Both of the synchronization methods, presented in detail, provide complimentary and consistent results, and are able to synchronize the CSC trigger primitives at the CSCTF. Synchronizing the CSCTF LCTs in this way corrects for known and unknown sources of error and asynchronization, which then increases trigger efficiency and quality of the muon tracks. For these reasons, a check of the synchronization of the CSCTF LCTs should be performed after any upgrades are implemented. In the future this note will provide a template for synchronization purposes.

References

[1] D. Acosta et al., "Synchronization of CSC Trigger Primitives Arriving at the CSC Track Finder", June, 2009.

[2] R. Breedon et al., "CSC Strip, Wire, Chamber, and Electronics Conventions", *Internal Note* (March, 2007).

[3] P. Everaerts and E. Juska, "P5 Timing", September, 2014.

[4] F. James, "MINUIT: Function Minimization and Error Analysis". CERN, d506 edition, 1998.

[5] R. Brun and F. Rademakers, "ROOT An object oriented data analysis framework", *Proceedings AIHENP'96 Workshop, Lausanne, Sep. 1996, Nucl. Inst. & Meth. in Phys. Res. A* **389** (1997) 81, doi:http://dx.doi.org/10.1016/S0168-9002(97)00048-X.

[6] M. James, "The Generalised Inverse", *The Mathematical Gazette* **62** (1978), no. 420, 109.

[7] CERN, "TDecompSVD". https://root.cern.ch/root/html/TDecompSVD.html.

[8] Particle Data Group Collaboration, "Review of Particle Physics", *Chin. Phys.* **C38** (2014) 090001, doi:10.1088/1674-1137/38/9/090001.

[9] P. R. Bevington and D. K. Robinson, "Data Reduction and Error Analysis for the Physical Sciences". McGraw-Hill, 1992.

A Matrix Minimization as Presented by the Particle Data Group

For completeness a method for calculating the Δ_i values from the Particle Data Group's (PDG) *Review of Particle Physics* [8] is presented, and shown to be equivalent to the result outlined in section 3.4. This is also the method presented in the 2009 synchronization note [1], so is also displayed here for consistency.

The form of the chi-squared function used in reference [8] is

$$\chi^2 = \sum_i \left(\frac{y_i - \mu(x_i;\theta)}{\sigma_i} \right)^2. \tag{14}$$

This is a very general chi-squared wherein y_i is the mean of the measured value at point x_i, θ is the vector of the parameters that are being varied with the purpose of minimizing equation 14, σ_i is the error on y_i, and $\mu(x_i,\theta)$ is the theoretical mean of y_i. In order to minimize equation 1 using the PDG method, it must be cast in the form of equation 14. To do this, y_i may be interpreted as m_i, θ will be signified by Δ, and $\mu(x_i;\Delta)$ will be defined as

$$\mu(x_i;\Delta) = \Delta_{i+1} - \Delta_i. \tag{15}$$

When the m_i are not independent, as is the case of the CSCTF LCT synchronization variables, but instead have some covariance matrix $V_{ij} = \sigma_{ij}^2$ equation 14 is replaced by

$$\chi^2 = (m - \mu(\Delta))^T V^{-1} (m - \mu(\Delta)), \tag{16}$$

where $m = (m_1, m_2, \ldots, m_N)$ is the column vector composed of the m_i variables, and $\mu(\Delta) = (\Delta_2 - \Delta_1, \Delta_3 - \Delta_2, \ldots, \Delta_1 - \Delta_N)$ is the column vector composed of the $\mu(x_i;\Delta)$ values. The problem is further restricted to the case where $\mu(x_i;\Delta)$ is a linear combination of the Δ_i variables, i.e.:

$$\mu(x_i;\Delta) = \sum_{j=1}^{m} \Delta_j h_j(x_i), \tag{17}$$

where $h_j(x)$ is m linearly independent functions. The exact identities of these $h_j(x)$ are not important because a matrix $H_{ij} = h_j(x_i)$ can be defined such that $\mu(\Delta) = H\Delta$. From this definition and equation 15, it follows that

$$H = \begin{bmatrix} -1 & 1 & 0 & \cdots & \cdots \\ 0 & -1 & 1 & 0 & \cdots \\ & \vdots & & \ddots & \\ 1 & 0 & \cdots & 0 & -1 \end{bmatrix}. \tag{18}$$

Minimizing the chi-squared in equation 16 by setting its derivatives with respect to the Δ_i variables equal to zero gives the vector of desired synchronization timing constants, from reference [8],

$$\Delta = (H^T V^{-1} H)^{-1} H^T V^{-1} m, \tag{19}$$

which can be rewritten as

$$(H^T V^{-1} H)\Delta = H^T V^{-1} m. \tag{20}$$

As mentioned in section 3.4.1, the value of the covariance between each m_i is assumed to be zero, making every off-diagonal entry of V equal to zero as well. For simplicity, and to avoid having to find an additional pseudoinverse when an overlap region is missing data (i.e. $\sigma_i^2 = 0$), V will be explicitly defined as

$$(V^{-1})_{ij} = \begin{cases} \frac{1}{\sigma_i^2} & \text{if } i = j \text{ and } \sigma_i^2 \neq 0 \\ 0 & \text{otherwise} \end{cases}. \tag{21}$$

When V is defined in this way, equations 14 and 16 are equivalent. With H and V defined, equation 20 can be written as

$$\underbrace{\begin{bmatrix} \frac{1}{\sigma_1^2}+\frac{1}{\sigma_N^2} & -\frac{1}{\sigma_1^2} & 0 & \cdots & -\frac{1}{\sigma_N^2} \\ -\frac{1}{\sigma_1^2} & \frac{1}{\sigma_1^2}+\frac{1}{\sigma_2^2} & -\frac{1}{\sigma_2^2} & 0 & \cdots \\ \vdots & \ddots & & \ddots & \cdots \\ -\frac{1}{\sigma_N^2} & 0 & \cdots & -\frac{1}{\sigma_{N-1}^2} & \frac{1}{\sigma_{N-1}^2}+\frac{1}{\sigma_N^2} \end{bmatrix}}_{H^T V^{-1} H} \underbrace{\begin{bmatrix} \Delta_1 \\ \Delta_2 \\ \vdots \\ \Delta_N \end{bmatrix}}_{\Delta} = \underbrace{\begin{bmatrix} -\frac{1}{\sigma_1^2} & 0 & \cdots & \frac{1}{\sigma_N^2} \\ \frac{1}{\sigma_1^2} & -\frac{1}{\sigma_2^2} & 0 & \cdots \\ \vdots & & \ddots & \cdots \\ \vdots & 0 & \frac{1}{\sigma_{N-1}^2} & -\frac{1}{\sigma_N^2} \end{bmatrix}}_{H^T V^{-1}} \underbrace{\begin{bmatrix} m_1 \\ m_2 \\ \vdots \\ m_N \end{bmatrix}}_{m} \tag{22}$$

Row i of this equation can be written as

$$\Delta_i\left(\frac{1}{\sigma_i^2}+\frac{1}{\sigma_{i-1}^2}\right) - \frac{\Delta_{i+1}}{\sigma_i^2} - \frac{\Delta_{i-1}}{\sigma_{i-1}^2} = \frac{m_{i-1}}{\sigma_{i-1}^2} - \frac{m_i}{\sigma_i^2}. \tag{23}$$

Multiplying through by σ_{i-1}^2 and σ_i^2 gives

$$-\sigma_i^2\Delta_{i-1} + (\sigma_{i-1}^2+\sigma_i^2)\Delta_i - \sigma_{i-1}^2\Delta_{i+1} = \sigma_i^2 m_{i-1} - \sigma_{i-1}^2 m_i, \tag{24}$$

which is the same as equation 3 from section 3.4. Therefore, the two matrix methods presented are equivalent. Uncertainties for the nominal values determined from this minimization method may be calculated in the same way as the method outlined in section 3.4.1.